



Pantoprazole Sodium Sesquihydrate Complexes: Synthesis, Characterization, Potentiometric Determination and DNA interaction

Y. M. ISSA¹, W. H. HEGAZY^{2*}, W. N. EL-SAYED^{2,3} and H. I. AHMED²

¹Department of Chemistry, Faculty of Science, Cairo University, Giza, Egypt.

²Department of Chemistry, Faculty of Science, Suez University, Suez, Egypt

³Chemistry Department, Faculty of Science and Arts, University of Jeddah, Alkamel, Kingdom of Saudi Arabia.

*Corresponding author E-mail: wael.hegazy@suezuniv.edu.eg

<http://dx.doi.org/10.13005/ojc/320234>

(Received: February 12, 2016; Accepted: March 09, 2016)

ABSTRACT

The synthesis and characterization of solid complexes for pantoprazole sodium sesquihydrate (PNZ) with Cd(II), Hg(II) and Zn(II) metals in molar ratios M:L = 1:2 was studied. The complexes are stable in the solid state and are soluble only in DMF and DMSO. The metal complexes were characterized by elemental analysis, molar conductivity measurements, magnetic susceptibility, UV spectrophotometry, IR, Mass spectra, TGA/DTG analysis. Potentiometric measurements for these metal complexes were studied.

Keywords: Pantoprazole, complexes, potentiometry, Proton Pump Inhibitors, DNA interaction.

INTRODUCTION

Pantoprazole sodium sesquihydrate is benzimidazole derivative which have biological activity to inhibit gastric acid secretion¹. Pantoprazole acts as good ligand as it has several coordination modes²⁻⁴. Many drugs enhance its pharmacological and toxicological properties by their complexation with metal ions. Cd(II), Hg(II) and Zn(II)⁵. In this paper, several techniques were used to characterize

the prepared pantoprazole complexes. DNA interaction of these complexes was given.

EXPERIMENTAL

Solid complexes

All complexes were prepared according to the following procedure. The pantoprazole ligand (0.5 mmol) is dissolved in 10 cm³ H₂O. The metal salt (0.25 mmol) dissolved in 10 cm³ H₂O

is added dropwise with continues stirring to the ligand solution. The formed precipitate was filtered, washed with hot water and dried. Synthesized solid complex were characterized by elemental analysis, IR, mass spectrometry, electrical conductivity, magnetic susceptibility, UV spectroscopy and thermal analysis.

Physical measurements

The electronic absorption spectra were obtained in 10^{-5} mol/L DMF solution in 1 cm quartz cell using Shimadzu-1601PC UV-Visible automatic recording spectro-photometer. The CHNS elemental analysis was estimated using Thermo Flasha Eager 300. The infrared spectra were recorded as KBr discs in the 400-4000 cm^{-1} range using perkin Elmer 1650 FT-IR instrument. TGA were obtained using a Shimadzu DTG-60H in a dynamic air atmosphere (30 cm min^{-1}) at a heating rate of $10 \text{ }^\circ\text{C min}^{-1}$. Conductivity of the dissolved complexes were carried out at room temperature on freshly prepared 10^{-3} mol/L DMF solutions using Jenco Model 1671 Dual Display Bench Top instrument pH/ORP (redox)/conductive. Magnetic susceptibility measurements were carried out using the modified Gouy method⁶ on MSB-MK1 balance at room temperature using mercuric (II) tetrathiocyanatocobaltate(II). The effective magnetic moment μ_{eff} per metal atom was calculated from the expression $\mu_{\text{eff}} = 2.83 \sqrt{x} \cdot T \text{ B.M.}$, where x is the molar susceptibility corrected using Pascal's constant for the diamagnetism of all atoms in the complexes. Mass spectra were done by AMD Intectra Gmb HDP10. Data system EI/8 Kv spectrometer.

Kinetic parameters

In order to assess the influence of the structural properties of the ligand and the type of metal on thermal behavior of the complexes, the order n and the heat of activation E at the various decomposition stages were determined from TGA and DTG thermograms using the Coats-Redfern equations in the following form⁷.

$$\ln \left[\frac{1 - (1 - \alpha)^{1-n}}{(1-n)T^2} \right] = \ln \left(\frac{AR}{\beta E} \right) \left[1 - \frac{2RT}{E} \right] - \left(\frac{E}{2.303RT} \right) \quad \text{for } n \neq 1 \quad \dots(1)$$

$$\ln \left[-\frac{\ln(1-\alpha)}{T^2} \right] = \ln \left(\frac{AR}{\beta E} \right) \left[1 - \frac{2RT}{E} \right] - \left(\frac{E}{2.303RT} \right) \quad \text{for } n = 1 \quad \dots(2)$$

Where: α is fraction of weight loss, T is temperature (K), n is order of reaction, A is pre-exponential factor, R is molar gas constant, E_a is activation energy, \hat{a} is heating rate.

The correlation factor r is computed using the least squares method for equations (1) and (2). Linear curves were drawn for values equal 0.5, 1, 1.5, 2, 2.5 and 3. The value of n which gave the best linear plot was chosen as the order parameter for the decomposition stage of interest and the heat of activation was calculated from its slope^{8,9}.

The activation entropy ΔS , the activation enthalpy ΔH and the free energy of activation ΔG were calculated using the following equations:

$$\Delta S = R \ln \left(\frac{Ah}{KT} \right) \quad \dots(3)$$

$$\Delta H = E - RT \quad \dots(4)$$

$$\Delta G = \Delta H - T\Delta S \quad \dots(5)$$

K and h are the Boltzman's and Plank's constants.

DNA Interaction

All the experiments involving the binding of complexes with CT-DNA were carried out in double distilled water and adjusted to pH 7.2. Absorption titration experiments were performed with fixed concentrations of the compounds (1×10^{-4} mol/L) with varying concentration of DNA (0–60 $\mu\text{mol/L}$). While measuring the absorption spectra, an equal amount of DNA was added to both the test solution and the reference solution to eliminate the absorbance of DNA itself. The values of the intrinsic binding constants K_b were calculated by regression analysis using the equation¹⁰.

$$[\text{DNA}]/(\epsilon_a - \epsilon_f) = [\text{DNA}]/(\epsilon_b - \epsilon_f) + 1/K_b (\epsilon_a - \epsilon_f)$$

where [DNA] is the concentration of CT-DNA in base pairs and ϵ_a , ϵ_f and ϵ_b are molar absorptivities of the apparent, free and bound metal complex, respectively and K_b is the equilibrium binding constant. In the plots of $[\text{DNA}]/(\epsilon_a - \epsilon_f)$ versus [DNA], K_b is given by the ratio of slope to the intercept.

Potentiometric study

All materials employed in the present investigation were of A.R. grade products. [amino succinic acid] $C_4H_7NO_2$ (Aspartic acid), [2-amino-propanoic acid] $C_3H_7NO_2$ (Alanine), [2-amino-3-imidazole propanoic acid] $C_6H_9N_3O_2$ (Histidine), $C_4H_9NO_3$ (Threonine), $C_3H_7NSO_2$ (Cysteine), and $C_9H_{11}NO_2$ (Phenylalanine), were purchased from Sigma-Aldrich Company and were used without purification. To account for preparation of metal ion amino acid solutions of exactly a 1:1 ratio, we also determined, by potentiometric pH titration, the molecular weight of these amino acids.

RESULTS AND DISCUSSIONS

Elemental analysis

The elemental analyses of the solid complexes of pantoprazole are recorded in Table

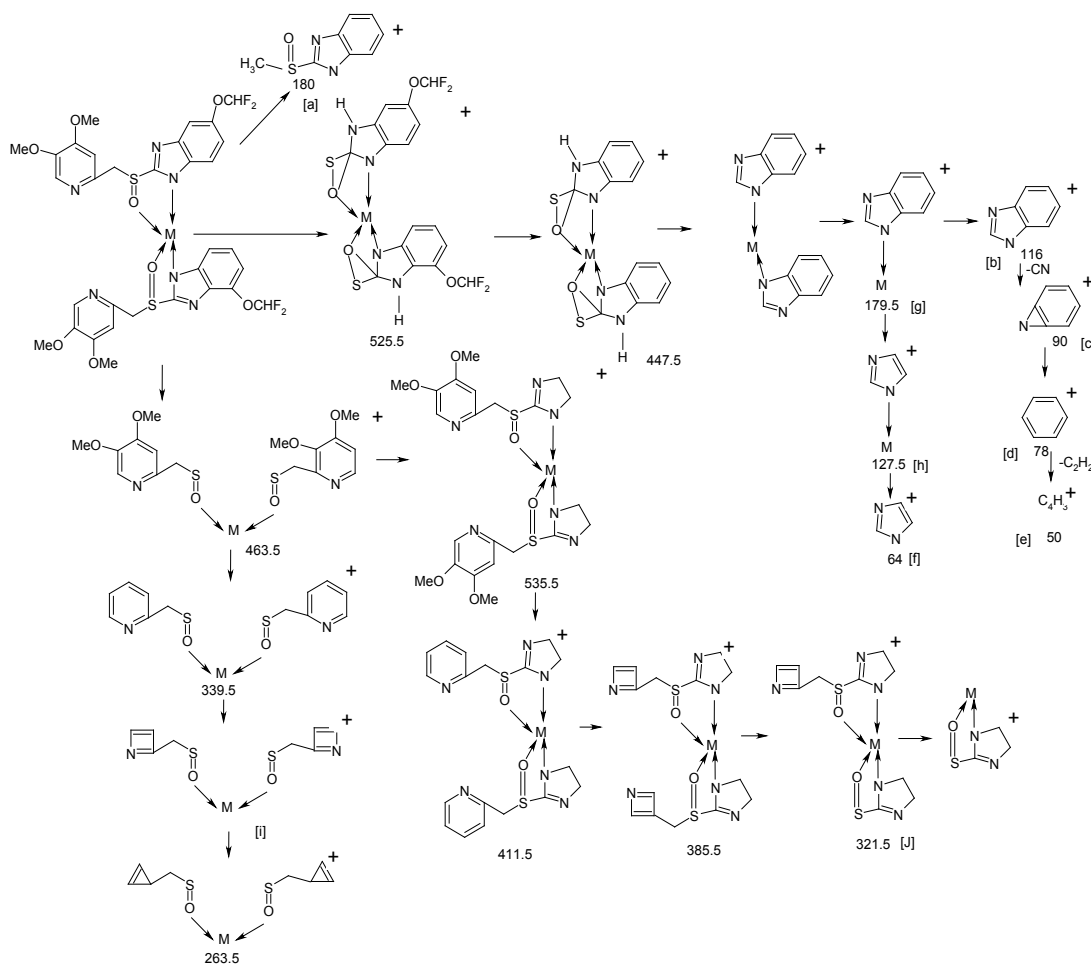
(1). It is clear that the formula of the Hg^{2+} and Zn^{2+} complexes may be represented as $[M(PNZ)(H_2O)Cl]H_2O$, while Cd^{2+} complex is represented as $[Cd(PNZ)_2(H_2O)_2]H_2O$.

Molar conductivity measurements

The complexes were dissolved in DMF and the molar conductivities of 10^{-3} mol/L of their solutions at 25 ± 2 °C were measured. Table (2) shows the molar conductance values of the complexes. It is concluded from the results that the complexes are found to have molar conductance values of 6–18.8 $\Omega^{-1} \text{ cm}^2 \text{ mol}^{-1}$ indicating that these complexes are non-electrolytes. It also, indicates the bonding of the chloride anion to the metal ions.

Electronic spectra measurements and magnetic susceptibility

The UV-Visible spectra of the ligand



Scheme 1: Fragmentation pattern for PNZ-complexes

and its complexes were recorded in DMF at room temperature. The electronic spectrum of ligand showed only one intense band at 34246 cm^{-1} , which was assigned to $n \rightarrow \pi^*$ transition of the C=N chromophore. The complexes of Zn(II), Hg(II) and Cd(II) is diamagnetic and have only one peak in the UV region. According to the empirical formula, Cd(II) complex has an octahedral geometry while both Zn(II) and Hg(II) have tetrahedral geometry.

IR spectra and mode of bonding

IR spectra for the ligand and its complexes are shown in Table (3). In the free ligand, the band at 1373 cm^{-1} is assigned to $\nu(\text{C-N})$. After complexation, this band is shifted to higher frequency in the three complexes. Shifting of the $\nu(\text{C-N})$ vibration is due to $\text{C-N} \rightarrow \text{M}^{2+}$ coordination¹¹. Characteristic band at 3498 cm^{-1} is assigned to presence of water in the ligand structure; similarly presence of coordinated water is confirmed by the presence of band at $3372\text{-}3440\text{ cm}^{-1}$ ¹². Coordinated water molecule is also noticed as a weak band at $815\text{-}820\text{ cm}^{-1}$ due to rocking mode while band at $450\text{-}630\text{ cm}^{-1}$ indicated

the presence of water of crystallization¹³. In addition, IR spectrum of the ligand revealed a sharp band at 1035 cm^{-1} due to $\nu(\text{S=O})$ of side chain, which is shifted to higher frequency after complexation in all complexes, suggesting that oxygen atom of the side chain also contributes to the complexation. New bands appeared in the spectra of the complexes at $633\text{-}733\text{ cm}^{-1}$, corresponding to $\text{O} \rightarrow \text{M}$ and $410\text{-}540\text{ cm}^{-1}$ due to the $\text{N} \rightarrow \text{M}$ vibrations which support the involvement of N and O atoms in complexation with metal ions under investigation¹⁴. Characteristic strong band at 1486 cm^{-1} is assignable to the stretching vibration of aromatic C=N group in benzimidazole ring that remained unchanged after complexation which confirmed the non-coordination of this group¹⁵. Another band appears at the spectra of Hg(II) and Zn(II) complexes at $865\text{-}900\text{ cm}^{-1}$ due to Cl^- vibration which support the involvement of Cl atom in complexation of these chelates. all these discussions indicate that the ligands are bidentate and coordinating via O, N atoms.

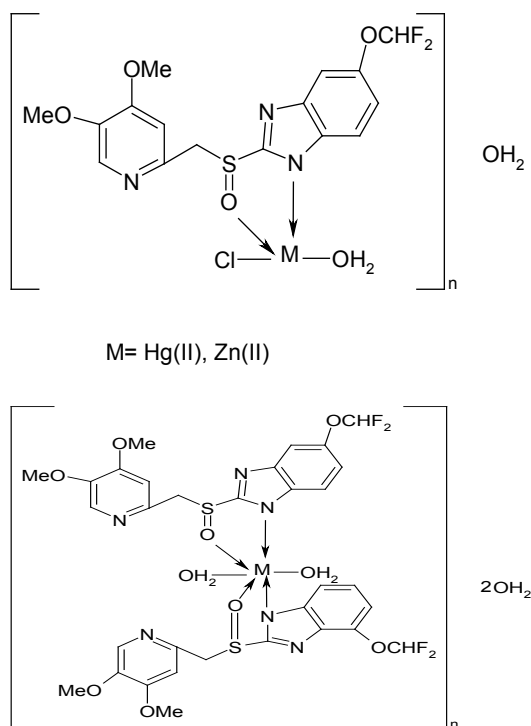
Mass spectra

The mass spectral data did not show any of the required molecular ion peaks, but it could be deduced through studying of the assigned fragmentation peaks. All complexes have the same fragmentation, which have the main fragments [a], [b], [c], [d], [e], [f] at $m/z = 180(4.5)$, $116(8.5)$, $90(10.2)$, $78(14)$, $50(50.3)$ and $64(36.2)$ (as fragments of ligand), which confirm the proposed structure of complexes. This was also confirmed by the appearance of a peak at $179.5(7.9)$, $127(2.8)$, $291.5(5.1)$ and $321(5.6)$ for fragments [g], [h], [i] and [j] respectively. The most prominent peaks were assigned as shown in the following fragmentation (Scheme.1).

Thermal analysis

The thermal behavior of the PNZ-Complexes was characterized using TGA/DTG method. The decomposition stages, temperature ranges and decomposition products as well as the found and calculated weight loss are given in Table (4). The activation energies and kinetic parameters were calculated using Coats-Redfern equation⁷ and the values are given in Table (5).

Cadmium complex undergo decomposition in four steps. Dehydration of the complex takes



Scheme 2: Complexes of Cd-PNZ, Hg-PNZ and Zn-PNZ

place in the 39-121°C range with DTG peak at 72°C associated with weight loss of 3.1% (Calcd. 3.86%). Coordination sphere decomposition for the cadmium complex is concerned with the elimination of the

coordinated water and partial decomposition of the ligand. It takes place with DTG maxima at 233°C in the 120.4-302.9°C range. The ligand is continued to decompose at maxima 306.5 and 421.7 °C in the

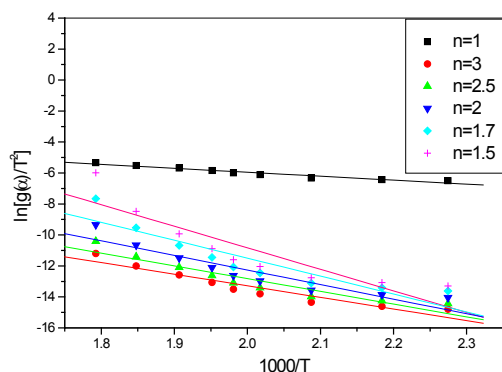


Fig. 1: Linearization curves of $[\text{Cd}(\text{PNZ})_2(\text{H}_2\text{O})_2]$ H_2O complex (first decomposition step)

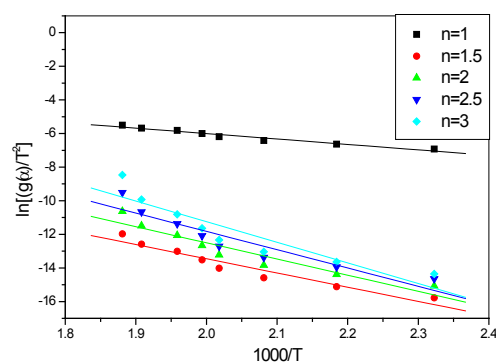


Fig. 2: Linearization curves of $[\text{Hg}(\text{PNZ})(\text{H}_2\text{O})\text{Cl}]\text{H}_2\text{O}$ complex (first decomposition step)

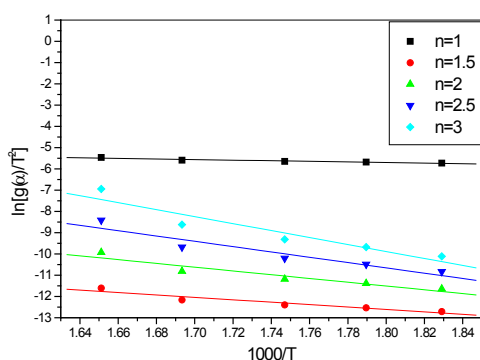


Fig. 3: Linearization curves of $[\text{Hg}(\text{PNZ})(\text{H}_2\text{O})\text{Cl}]\text{H}_2\text{O}$ complex (second decomposition step)

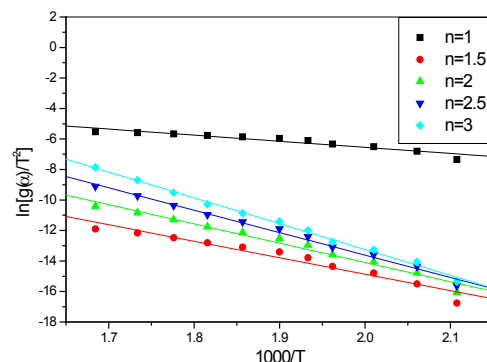


Fig. 4: Linearization curves of $[\text{Hg}(\text{PNZ})(\text{H}_2\text{O})\text{Cl}]\text{H}_2\text{O}$ complex (third decomposition step)

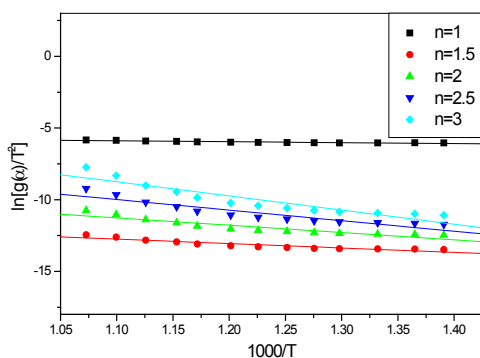


Fig. 5: Linearization curves of $[\text{Zn}(\text{PNZ})(\text{H}_2\text{O})\text{Cl}]\text{H}_2\text{O}$ complex (first decomposition step)

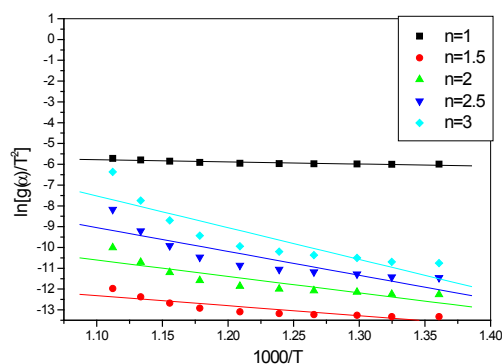


Fig. 6: Linearization curves of $[\text{Zn}(\text{PNZ})(\text{H}_2\text{O})\text{Cl}]\text{H}_2\text{O}$ complex (second decomposition step)

range of 302.9-388.7 and 388.7-801 °C, respectively with no definite final product since the decomposition process is not complete at 800 °C.

TGA/DTG curves of the mercury complex are characterized by three decomposition steps. The first step takes place in the 35.4-256.7 °C range with DTG peaks at 38.2 and 228°C. Observed mass loss is 33.6% against calculated one of 33.1% corresponding evolution of crystallization water, coordinated water, chloride ion and partial decomposition of the ligand. The ligand is continued to decompose at 256.7 °C and end with final decomposition at 398.4 °C. The final decomposition is attributed to the evaporation of Hg metal with

weight loss of 33.8% against calculated one of 33.6%. Carbon is remained as final product.

Thermal decomposition of zinc complex takes place in four stages. The first stage starts at 117.9-321.9 °C range. This was accompanied with mass loss of 30.3% (Calcd. 29.9%) with maximum DTG at 228.5 °C, which attributed to the volatilization of the hydrated water, coordinated water, chloride ion and partial decomposition of the ligand. The second decomposition stage takes place in the 322.9-425.5°C range with maxima at 410°C, which correspond decomposition of ligand. The third decomposition stage takes place at 426.4-506.4 °C range with maximum DTG at 491.6°C attributed to further decomposition of ligand with mass loss of 4.6% (Calcd. 4.4%). The final decomposition stage occurs in the range 506.9-797 °C with maxima at 603 and 781°C with no definite final product since the decomposition process is not complete at 800 °C.

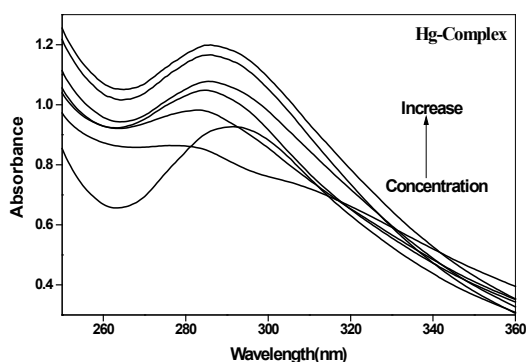


Fig. 7: Effect of concentration of DNA on the absorption band at $\lambda = 293$ nm (Hg-Complex = 1×10^{-4} molL $^{-1}$)

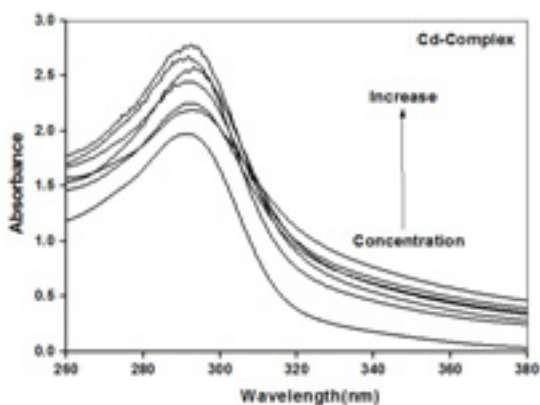


Fig. 8: Effect of concentration of DNA on the absorption band at $\lambda = 293$ nm (Cd-Complex = 1×10^{-4} molL $^{-1}$)

From the TGA curves, the order n , activation energy E , and pre-exponential factor A of the different thermal decomposition steps of the complexes have been elucidated by the method of Coats-Redfern⁷. Some examples of the linearization curves for the complexes, which were obtained, presented in Figs. (1-6). The values of correlation coefficients of linearization curves of the complexes and their reaction orders are given in Table (5). The activation energy E and enthalpy of activation ΔH of the three complexes are expected to increase proportional to decrease in their radii¹⁴. The activation energy of the

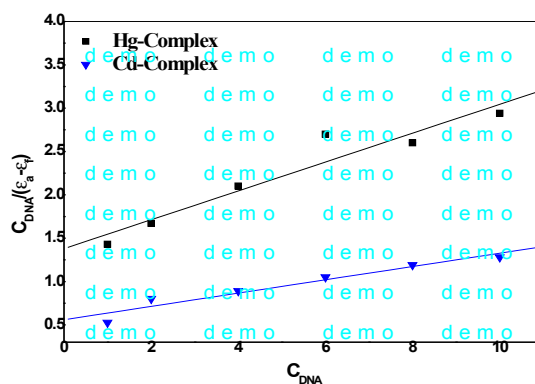


Fig. 9: Plot of $[DNA]/(\epsilon_a - \epsilon_e)$ versus $[DNA]$

tetrahedral $[\text{Zn}(\text{PNZ})(\text{H}_2\text{O})\text{Cl}]\text{H}_2\text{O}$ complex is higher than $[\text{Hg}(\text{PNZ})(\text{H}_2\text{O})\text{Cl}]\text{H}_2\text{O}$ complex.

The smaller the radius of metal ion, the easier the ligand approaches the central atom. As a result, metal-ligand interaction becomes stronger, the detachment of the link becomes more difficult and E values increase^{15,16}. The negative values of the entropies in the decomposition reactions of the complexes Table (5) indicates that the reactions are slower than normal¹⁷⁻¹⁹ and the activated complexes have more ordered structure than the reactants^{20,21}.

Based on the above analytical data and physicochemical properties, the following structures are proposed in which the metal ion is coordinated through C-N, sulphonyl groups S=O, the coordinated water and the coordinated anion.

DNA Interaction

UV-Vis Absorption spectra (Figs. 7,8) were obtained by titration of (1×10^{-5} – 1×10^{-4} M) complex solution with increasing concentration of DNA. In

absence of DNA, the spectrum is characterized by a peak at 293 nm. The absorbance of the peak increased gradually as DNA concentration increased.

The spectral changes reflect the corresponding changes in DNA in its conformation and structures after the drug bound to DNA. Intercalative mode of binding usually results in hypochromism and bathochromism due to strong stacking interaction between an aromatic chromophore and the base pairs of DNA. On the other hand, metal complexes which non-intercalatively or electrostatically bind with DNA may result in hyperchromism and hypsochromism. The absorption spectra show clearly that the addition of DNA to the complexes lead to strong hyperchromism accompanied by the slight hypsochromism to the $[\text{DNA}]/[\text{complex}]$ (Fig. 9). Obviously, these spectral characteristics suggest that all the complexes interact with DNA via electrostatically with the base pairs of DNA²².

Table 1: Analytical data and magnetic moments of the PNZ and its complexes

Compound	Chemical formula	% Found (Calcd.)				M	$\mu_{\text{eff.}}$ (298°K) (B.M)
		C	H	N	S		
PNZ	$\text{C}_{16}\text{H}_{14}\text{F}_2\text{N}_3\text{O}_4\text{S.Na.1.5H}_2\text{O}$	43.2 (44.4)	3.0 (3.24)	9.4 (9.7)	6.5 (7.4)	—	
Zn-PNZ	$[\text{Zn}(\text{PNZ})(\text{H}_2\text{O})\text{Cl}]\text{H}_2\text{O}$	36.3 (36.97)	3.2 (3.47)	8 (8.08)	5.8 (6.16)	12.1 (12.5)	Diamagnetic
Cd-PNZ	$[\text{Cd}(\text{PNZ})_2(\text{H}_2\text{O})_2]\text{H}_2\text{O}$	40.7 (41.24)	3.4 (3.65)	8.9 (9.02)	6.5 (6.87)	11.8 (12.07)	Diamagnetic
Hg-PNZ	$[\text{Hg}(\text{PNZ})(\text{H}_2\text{O})\text{Cl}]\text{H}_2\text{O}$	28.5 (29.34)	2.6 (2.75)	6.1 (6.42)	4.5 (4.89)	29.9 (30.65)	Diamagnetic

Table 2: Physical data of the PNZ ligand and its complexes

Compound	Chemical formula	M. Wt	% Yield	Color	Λ_m ($\Omega^{-1}\text{cm}^2\text{mol}^{-1}$)	Melting Point(°C)
PNZ	$\text{C}_{16}\text{H}_{14}\text{F}_2\text{N}_3\text{O}_4\text{S.Na.1.5H}_2\text{O}$	432.38	82	Off white	—	137
Zn-PNZ	$[\text{Zn}(\text{PNZ})(\text{H}_2\text{O})\text{Cl}]\text{H}_2\text{O}$	519.26	70	Off white	6	170
Cd-PNZ	$[\text{Cd}(\text{PNZ})_2(\text{H}_2\text{O})_2]\text{H}_2\text{O}$	931.16	73	Faint brown	5.4	160
Hg-PNZ	$[\text{Hg}(\text{PNZ})(\text{H}_2\text{O})\text{Cl}]\text{H}_2\text{O}$	654.47	62	Faint red	7	155

In order to evaluate quantitatively the DNA-binding strength, the intrinsic DNA-binding constants, K_b of the complexes have been estimated to be in the range [0.121– 0.382 mol/L] and is are listed in the Table (6).

pH-metric Measurements

The formation of various 1:1:1 ternary complex species are inferred from the potentiometric-pH titration curves. Initial estimates of the stability constants of the resulting species and the acid dissociation constants of pantoprazole, and amino acids have been refined with the HYPERQUAD computer program²³. The quality of the fit during this refinement was judged by the values of the sample standard deviations and the goodness of fit χ^2 (Pearson's Test). At $\sigma_E = 0.1$ mV (0.001 pH error) and $\sigma_V = 0.005$ cm³, the values of S in different sets of titrations were between 1.0 and 1.7 and χ^2 was between 12.0 and 13.0. The scatter of residuals ($E_{obs} - E_{calc}$) versus pH reasonably random, without any significant systematic trends, thus indicating a good fit of the experimental data of the expected model systems under our experimental conditions. Furthermore, the formation constants values of the different 1:1 metal ion- amino acids have been determined under identical conditions. This is made with the aim to compare the stability of the formed 1:1:1 ternary complex with of the corresponding 1:1 binary metal complexes.

All the initial estimates of the formation constants of the different binary and ternary complexes formed in the present investigation have been refined using HYPERQUAD computer program.

$$K_{M(PNZ)(AA)} = \frac{[M_p(PNZ)_q(AA)_r]}{[M_p(PNZ)_q][AA]^r}$$

Which refers to the addition of amino acids to the binary complex $M_p(PNZ)_q$. The overall complexation reaction involving protonation is,



$$\beta_{pqrs} = \frac{[M_p(PNZ)_q(AA)_r(H)_s]}{[M]^p [PNZ]^q [L]^r [H]^s}$$

Which, AA = amino acids, PNZ = Pantoprazole, M = Cd(II), Zn(II).

The data points collected in the pH range 3.0-11.0 were used for the calculations and refinements. The formation constants of all the binary and the ternary complexes studied are given in Tables (7,8).

The pH-metric titration curves in case of PNZ ligand before the acid curve indicating that in acidic solutions each molecule of the ligand is in association with one equivalent of proton. This proton should be attached with the lone pair of electrons present on the nitrogen of the ring in the case of PNZ. PNZ shows one step acid dissociation due to deprotonation of one secondary amine group.



Representative set of experimental titration curves, obtained according to the sequence for different M-PNZ reveals that below pH 7.5 formation of different M-PNZ binary complexes take place. This is clear from the appeared divergence of each of the 1:1 binary M-PNZ titration curve from that of the corresponding free PNZ curve. Binary complexes are stable up to pH 5-8 in case of different metal ions. Hydrolysis of the complexes leads to the formation of hydroxo-complex species. The nature of the pH titration curves indicates that stepwise complex formation take place through deprotonation of secondary amine group. The acid dissociation constant value are for pantoprazole ($pK_a = 6.2 \pm 0.02$)⁵. The acid dissociation constant values for amino acids are in good agreement with those found in the literature²⁴.

Of the 20 α -amino acids that commonly occur in proteins; about half contain side chain donor atoms that are at least potentially capable of forming a chelate ring with metal ion bound at the α -amino nitrogen. If the α -amino and α -carboxylate groups that occur in the free amino acids also chelate the metal ion, then two chelate rings will be formed.

The order of stability constants of M + PNZ + Alanine is Cd > Zn.

Phenylalanine, as its name indicates, contains a phenyl ring attached in place of one of the

Table 3: IR spectral data of the PNZ and its complexes (cm⁻¹)

Compd.	OH (str)	CH ₃ (str)	C=C (str)	C=N (str)	C-N (str)	C=C (str)	C-O (str)	C-F (str)	S=O (str)	O-H (bend)	M-N	M-O	Water of crystallization (Rocking mode)
Ligand	3498	3376 (assym) 3190 (sym)	1590	1486	1373	1298	1228 (assym) 1166 (sym)	1116	1035	—	—	—	—
Zn-Complex	3408	3088 (assym) 2984 (sym)	1585	1484	1423	1299	1231 (assym) 1172 (sym)	1119	1064	817	865	539	687
Cd-Complex	3411	3095 (assym) 2990 (sym)	1587	1490	1408	1303	1237 (assym) 1171 (sym)	1121	1066	820	—	410	683
Hg-Complex	3440	3079 (assym) 2946 (sym)	1619	1501	1437	1323	1264 (assym) 1173 (sym)	1122	1077	817	930	532	712

Table 4: TGA and DTG data of the PNZ and its complexes

Compound	Temp. range °C	DTG °C	Mass loss%		Process	Product	Residue % and type Found (Calcd.)
			Found	Calcd.			
[Zn(PNZ)(H ₂ O)Cl]H ₂ O	117.96-321.99	228.53	30.27	29.97	Dehydration+Coordination sphere partial decomposition	2H ₂ O + Cl + 0.22 Ligand	Not complete
	322.96-425.49	410	7.09	7.36	Coordination sphere partial decomposition		
	426.41-506.41	491.64	4.646	4.42	Ligand partial decomposition	0.1 Ligand	
	506.9-797.41	603.34-781.4	27.49	27.25	Ligand partial decomposition	0.06 Ligand 0.37 Ligand	
	39.22-121.1	72	3.1	3.86	Dehydration+Coordination	2H ₂ O	Not complete
[Cd(PNZ) ₂ (H ₂ O) ₂]H ₂ O	121.1-302.91	233.1	32.26	32.29	sphere partial decomposition		
	302.91-388.77	306.51	5.94	5.75	Coordination sphere partial decomposition		
	388.77-801.09	421.67	20.93	20.53	Ligand partial decomposition	H ₂ O + 0.42 Ligand	
	35.36-256.77	38.24	33.56	33.1	Ligand partial decomposition	0.15 Ligand 0.43 Ligand	
	256.77-398.45	347.78	31.45	31.55	Dehydration+Coordination sphere partial decomposition	2H ₂ O + Cl	1.83 Carbon (1.75)
[Hg(PNZ)(H ₂ O)Cl]H ₂ O	398.45-680.02	588.44	33.814	33.57	Coordination sphere partial decomposition		
	256.77-398.45	347.78	31.45	31.55	Final decomposition	0.54 Ligand 0.05Ligand + Hg	

hydrogen of alanine. The order of stability constants of M + PNZ + Phenylalanine is Zn > Cd.

Aspartic acid contains two acidic side chains. This amino acid is often called aspartate to emphasize that its side chain is usually negatively charged at physiological pH. The order of stability constants of M + PNZ + Aspartic acid is Cd > Zn .

The amino acid histidine in its dicationic form contains four acidic protons. As the pH increased the successive pKa values for proton removal are carboxylic acid imidazolium. -N(3)-H,

side chain ammonium imidazole -N(1)-H. The imidazole (1)-NH is very weakly acidic (pKa = 14.4) and thus it does not dissociate in the measurable pH range. It has been argued strongly that metal ion binding on the aromatic imidazole ring occurs only at pyridine nitrogen, as the energy required for binding to occur at a pyrrole nitrogen is prohibitive²⁵. The order of stability constants of M + PNZ + Histidine is Zn > Cd.

Threonine contains aliphatic hydroxyl group. It can be thought of as hydroxylated version of valine with hydroxyl group in place of one of the valine

Table 5: Kinetic parameters for the first decomposition step of the PNZ-complexes

Comp.	Step	E	A	n	R	ΔH	ΔG	ΔS
[Zn(PNZ)(H ₂ O)Cl]H ₂ O	1	324.2186	1.03E+16	3	0.9977	320.0488	291.3221	57.2781
	2	92.07861	3432.793	1.5	0.8861	83.31232	281.2472	-187.723
[Cd(PNZ) ₂ (H ₂ O) ₂]H ₂ O	1	48.86083	859168.6	1.5	0.9717	44.65311	113.3337	-135.706
[Hg(PNZ)(H ₂ O)Cl]H ₂ O	1	61.81923	3828334	1	0.9772	57.65342	119.3837	-123.199
	2	26.67542	36056564	1	0.9651	21.51425	87.52501	-106.335
	3	189.056	57501102	3	0.9273	181.894	272.4992	-105.179

E, ΔH, ΔG in KJ.mol⁻¹

ΔS in J.mol⁻¹.k⁻¹

A in S⁻¹

Table 6: The Binding constant of complexes with DNA

Complex	Binding constant (Kb)	R	SD
Hg-PNZ	0.121	0.9596	0.1904
Cd-PNZ	0.137	0.9685	0.0769

R = Correlation coefficients

SD = Standard deviations

methyl groups. The hydroxyl groups of threonine make them much more hydrophilic and reactive than valine²⁶. As the alcoholic hydroxy group is so weakly acidic (pKa > 14) that it does not undergo dissociation. The order of stability constants of M + PNZ + Threonine is Zn > Cd.

Cystein contains three dissociable protons, the last two of these deprotonations, those of the ammonium and the thiol groups take place

Table 7: Formation constants for the binary M + amino acids (AA) and M-PNZ ligand complexes at 25 ± 0.1°C and I = 0.1 mol.L⁻¹ KNO₃

Metal Ions	log _M (Ala)	log _M (Phe)	Log _M (Asp)	log _M (Thr)	Log _M (His)	log _M (Cys)	Log _M (PNZ)
Cd (II)	4.12± 0.02	4.11± 0.03	5.86± 0.02	4.16± 0.02	3.98± 0.04	8.89± 0.02	6.21± 0.03
Zn (II)	5.81± 0.02	4.96± 0.02	6.97± 0.02	4.9± 0.02	4.94± 0.02	8.45± 0.03	7.15± 0.02

Table 8: Formation Constants for M + Pantoprazole (PNZ) + Amino Acids (AA) 1:1:1 Ternary Complexes at 25.0 ± 0.1°C and I = 0.1 mol.L⁻¹

Metal ion	log _{M(Ala)(PNZ)}	log _{M(Phe)(PNZ)}	Log _{M(Asp)(PNZ)}	log _{M(Thr)(PNZ)}	Log _{M(His)(PNZ)}	log _{M(Cys)(PNZ)}
Cd (II)	15.47 ^b ± 0.02	2.18 ^a ± 0.02	19.11 ^b ± 0.02	1.96 ^a ± 0.02	1.56 ^a ± 0.02	19.58 ^b ± 0.02
Zn (II)	3.91 ^a ± 0.02	3.59 ^a ± 0.02	17.83 ^b ± 0.03	3.91 ^a ± 0.02	2.89 ^a ± 0.02	18.29 ^b ± 0.03

in overlapping processes. Cystein is typical ambidentate ligand, the possible metal binding sites are different in nature. COO⁻ is rather hard, S⁻ is fairly soft and NH₂ is borderline. The -SH and -NH₃⁺ groups have relatively high pKa values, and the sulfur atoms behaves as bridging ligands. Thus a great variety of metal complexes may be formed, including protonated and polynuclear complexes with monodentate and different bidentate and tridentate bonding modes. The order of stability constants of M + PNZ + Cystein is Cd > Zn .

The observed different orders may be attributed to different types of interactions depending on metal ion different geometrical behavior during the formation of binary and ternary complexes in solution.

CONCLUSION

From elemental analysis it can be concluded that the formula of the Zn²⁺ and Hg²⁺ complexes can

be represented as [M(PNZ)(H₂O)Cl]H₂O, while Cd²⁺ represented as [Cd(PNZ)₂(H₂O)₂]H₂O, the molar conductance for the complexes were measured in DMF and showed that PNZ-complexes are non-electrolytes. From magnetic susceptibility and UV spectroscopy it's found that Zn-PNZ, Cd-PNZ and Hg-PNZ complexes are diamagnetic where Zn and Hg have tetrahedral geometry, while Cd have octahedral geometry. IR spectra for ligand and its complexes showed that the pantoprazole act as bidentate ligand which form complexes with metals through C-N and S=O groups, also the spectra showed new peaks due to M-N and M-O which confirmed the involvement of N and O atoms in complexation with metal ions. The mass spectral data showed that three complexes formed with molar ratio M:L = 1:2. Thermal analysis showed the different decomposition stage of the metal complexes, which appear the presence of water of hydration in all complexes. The activation energy E and enthalpy of activation ΔH of the complexes are expected to increase proportional to decrease in their radii.

REFERENCES

1. Yogita, B.; Om, S. *Bioorg. Med. Chem.* **1995**, *20*, 6208–6236.
2. Suman, M.; Supriya, D.; Bharti, J. *RJPBCS* **2010**, *1*, 394-400.
3. Mohamed; G. G.; Ibrahim, N. A.; Attia, H. A. *Spec. chim. Acta A* **2009**, *72*, 610–615.
4. Tiwari, C. R. *Search Res.* **2011**, *3*, 24-28.
5. Tiwari, C. R. *JERAD* **2012**, *6*, No. 3A.
6. Figgis, B. N.; Lewis, J.: in Lewis, J.; Wilkins, R. G. (Eds.) **1960** *Magnetochemistry of complex compounds in Modern Coordination chemistry*, Interscience, New York.
7. Coats, A.W.; Redfern, J. P. *Nature* **1964**, *68*, 201.
8. Cotton, F. A.; Wilkinson, G.; Murillo, C. A.; Bochmann, M. *Advanced Inorganic Chemistry, Sixth Ed.* **1999** Wiley, New York.
9. Koley M. K.; Sivasubramanian S. C.; Varghese B.; Manoharan P. T.; Koley A. P. *Inorg. Chim. Acta* **2008**, *361*, 1485.
10. Wolfe A.; Shimer G. H.; Meehan T. *Biochem.* **1987**, *26*, 6392.
11. Mohamed, G. G.; El-Gamel, N. E. A.; Nour El-Dien, F. A. *Synth. React. Inorg. Met.-Org. Chem.* **2001**, *31*, 347.
12. Kohout, J.; Hvastijova, M.; Kozisek, J.; Diaz, J. G.; Valko, M.; Jager, L.; Svoboda, I. *Inorg. Chim. Acta* **1999**, *287*, 186.
13. Uçan, S.Y.; Uçan, M.; Mercimek, B. *Synth. React. Inorg. Met.-Org. Chem.* **2005**, *35*, 417-

- 421.
14. Sari, N.; Gurkan, P.; Arslan, S. *Transit. Met. Chem.* **2003**, *28*, 468-474.
15. Shyamala, B. S.; Lakshmi, P. V. A.; Raju, V. J. *J. Sci. Res.* **2010**, *2*, 525–537.
16. Silverstein, R. M.; Webster F. X. *Spectrometric identification of organic compounds* **2007** Wiley interscience, India, Delhi, 102.
17. Sallam S. A. *Trans. Met. Chem.* **2006**, *31*, 46.
18. Sangari, H. S.; Sodhi, S. *Thermo Chim. Acta* **1990**, *171*, 49.
19. Styczen, E.; Warnke, Z.; Wyrzykowski, D. *Thermo Chim. Acta* **2007**, *454*, 84.
20. Indria, V.; Parameswaran, G. *J. Therm. Anal.* **1993**, *39*, 1417.
21. Frost, A. A.; Pearson, R. G. *Kinetics and Mechanism* **1961**, Wiley interscience, New York.
22. Nagababu, P.; Naveena, J.; Latha, L.; Prashanthi, Y.; Satyanarayana, S. *J. Chem. Pharm. Res.* **2009**, *1*, 238.
23. Gans, P.; Vacca, A. J. *Talanta* **1996**, *43*, 1739.
24. Martell, A. E; Smith, R. M. *Critical Stability Constants* **1975**, vol. 1 and 2, Plenum Press, New York.
25. Sundberg, R. J.; Martin, R. S. *Chem. Rev.* **1974**, *74*, 471.
26. Berg, J. M.; Tymoczko, J. L.; Stryer, L. *The Molecular Design of Life-Protein Structure and Function* **2003**, Biochemistry, Fifth Edition.